PREDICTING CYCLIC SHEAR STRENGTH DEGRADATION IN RC USING THE GENERAL CRACK COMPONENT MODEL

D. Ruggiero[1] & E. Merhi[1]

[1] EPFL (École Polytechnique Fédérale de Lausanne), Lausanne, Switzerland, david.ruggiero@epfl.ch

Abstract: *The shear behaviour of reinforced concrete subjected to seismic loading remains an important and open topic in structural engineering research. Experimental evidence has demonstrated that reversed cyclic loading of concrete panels can cause a shear strength reduction of more than 20% even in regions where the longitudinal reinforcement is not expected to yield. This behaviour is well-captured by the General Crack Component Model (GCCM), a mechanics-based formulation that explicitly considers the constitutive behaviour and kinematics of cracks in reinforced concrete using a series-parallel system of bonded and unbonded regions. This paper examines the relationship between crack kinematics (width and slip) and shear failure under the assumptions of the GCCM, and demonstrates that a simple limit state for the local crack opening angle can be established as a function of the global crack angle and reinforcing ratios to serve as a means of assessment for cracked concrete. A parametric study is conducted using the GCCM to predict the degree of shear strength reduction expected under different cyclic loading conditions and mechanical reinforcing ratios, identifying regimes in which the effects of reversed cyclic loading may be most detrimental*.

1 Introduction

1.1 Background

The shear behaviour of reinforced concrete (RC) has been extensively studied over the past decades. To avoid brittle failure mechanisms that can potentially lead to significant human and economic losses, many mechanical models have been developed to accurately characterize the response of RC structures. While these methods now form the basis of most structural codes, the inherent uncertainties and complexity of RC behaviour still make predictions challenging, as highlighted by the degree of scatter in recent blind competitions (Collins, Bentz, Quach, & Proestos, 2015; Zhai, Chen, Worsfold, & Moehle, 2022).

RC structures in practice can be subjected to cyclic loading that further complicates their response. Although reversed cyclic loading is of particular interest in the field of earthquake engineering, loading and unloading cycles can also be caused by redistribution of forces due to nonlinearity or changing load ratios. Indeed, any robust structural model should have the capability to encapsulate cyclic loading effects, enabling its integration into a general analysis framework.

Within the seismic engineering domain, significant research has been conducted to date into the reversed cyclic shear behaviour of RC elements. In the context of capacity design, the goal is to avoid shear failure within the highly strained plastic hinge regions. As a result of this research, practical recommendations have entered design codes that limit the shear strength within plastic hinge regions (Canadian Standards Association, 2019). However, research has shown that a reduction in shear strength of at least 20% can also occur in non-hinging regions subjected to cyclic loading (Ruggiero, Bentz, Calvi, & Collins, 2016); therefore, it is important to determine the possible extent of this strength degradation and understand the mechanisms that cause it.

In particular, a general framework is required to assess the residual capacity of structures that have been damaged by cyclic loading. Assessment of existing structures will be a necessary and important endeavour over the coming decades, as most existing RC infrastructure built during the post-war era is now reaching its design service life. To efficiently allocate resources, engineers need tools that allow them to efficiently assess cracked RC structures subject to any combination of loads.

To date, the assessment of RC structures has primarily been based on procedures that involve comparing crack data, obtained through visual inspections, with predefined limits found in structural codes, which typically vary from country to country. Such a qualitative approach, while being very simple to implement, is dependent on the experience of the inspector, and does not allow the engineer to establish any connection between the observed damage and the reserve capacity of a structure (Ryan, Mann, Chill, & Ott, 2012; Zaborac, Athanasiou, Salamone, Bayrak, & Hrynyk, 2020). A rational alternative founded in structural mechanics will be necessary to allow quantitative assessment of large inventories of RC structures.

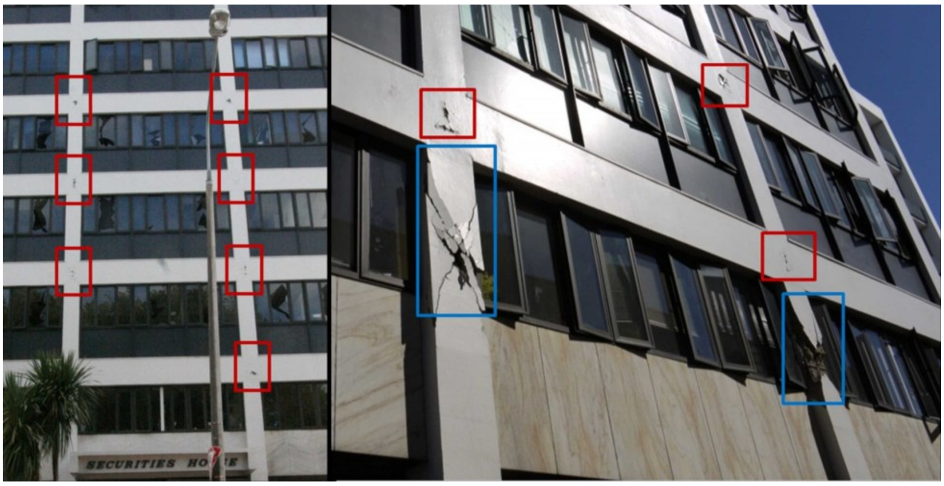

Figure 1. Building in Christchurch after 2011 earthquake, showing beam-column joints (red) and columns (blue) with reversed cyclic damage (Ruggiero, 2015).

1.2 Literature Review

Over the past years, many new methods have become increasingly available, with varying degrees of success, for estimating the capacity of cracked RC elements. These methods range from finite element analysis (Palermo & Vecchio, 2007; Červenka, Červenka, & Laserna, 2018) and empirical tools (Birrcher, et al., 2009; Larson, Gomez, Garber, Bayrak, & Ghannoum, 2013) to theoretical models based on fracture mechanics (Hillerborg, Modéer, & Petersson, 1976; Sain & Chandra Kishen, 2007; Wang, Shi, & Nakano, 2013) and mechanical approaches (Zhu, Wanichakorn, Hsu, & Vogel, 2003; Campana, Fernandez Ruiz, Anastasi, & Muttoni, 2013; Mihaylov, Bentz, & Collins, 2013; Lantsoght, van der Veen, Walraven, & de Boer, 2016; Cavagnis, Fernández Ruiz, & Muttoni, 2017; Calvi, Proestos, & Ruggiero, 2018; Zaborac, Athanasiou, Salamone, Bayrak, & Hrynyk, 2020).

Each of these models has exhibited successes and limitations; it is difficult to find a single model which is appropriate for a wide range of structure types and loading conditions. In addition, very few methods have been developed to date which take into account all measurable information about existing cracks (namely, the crack opening vector and crack shape) for the purpose of assessment. Some methods using the measured crack shape have shown promise in assessing damage in concrete structures (Trandafir, Proestos, & Mihaylov, 2022); the next step is to incorporate measurements of crack slip and width into these predictions in order to refine them and reduce estimation uncertainty.

With the advent of new technological capabilities, measuring crack parameters, especially the geometry, crack widths, and slips, is becoming more accessible and automatable. Incorporating these crack parameters measured on-field into assessment mechanical models can provide insight and new means of calculating more accurately the reserve capacity of a cracked RC element.

1.3 Scope of this work

The General Crack Component Model (GCCM) is a mechanical model for reinforced concrete formulated to describe cyclic and reversed cyclic load paths (Ruggiero, 2015). The GCCM represents cracks as distinct elements, each with its stiffness, in addition to the stiffness of the concrete and steel. Furthermore, it enables the modeling of various loads and crack directions by examining the behaviour and kinematics of cracks in reinforced concrete through a series-parallel system of bonded and unbonded regions.

In this paper, the GCCM is utilized to assess the extent of shear strength reduction anticipated under multiple cyclic conditions and reinforcing ratios, aiming to identify the most detrimental regime. The relationship between crack kinematics (width and slip) and shear failure is studied, facilitating the establishment of a limit state for the local crack opening angle as a function of the global crack angle and reinforcing ratios. This limit can serve for assessing cracked RC, providing a threshold for the crack opening angle indicative of physical failure, as demonstrated by application to experimental results from the literature.

Based on the assumptions of the GCCM, once the weaker direction of reinforcement in a shear panel has yielded, then any amplitude of cyclic loading will eventually lead to failure based on a degradation of the crack tooth angle. A parametric analysis is conducted to identify the regimes where this degree of strength loss is most significant, and it is shown how the predictions of the GCCM can be used to generate a preliminary S-N curve to estimate number of cycles to failure at any level of load cycling.

2 The General Crack Component Model

2.1 Mechanical formulation

The General Crack Component Model (GCCM) is a framework for the analysis of cracked reinforced concrete that explicitly considers equilibrium, compatibility, and stress-strain behaviour at crack interfaces and within the continuum. A full account of the formulation is provided elsewhere by Ruggiero (2015) but the key features will be summarized here below.

At a high level, the main premise of the GCCM is that cracked concrete can be represented as a series system of two types of regions: unbonded regions around cracks, in which the reinforcement is taken to be perfectly unbonded from the concrete; and bonded regions, where the reinforcement is taken to be perfectly bonded to the concrete. In the unbonded regions compatibility between steel and concrete is enforced only at the boundaries; the steel and cracked concrete are treated as elements in parallel. The cracked concrete in the unbonded region is itself a series system of uncracked concrete and the crack. Thus, the crack is treated as an integral structural element in this model, with discrete displacements (slip and width) arising from interface stresses (shear and normal force).

The one-dimensional series-parallel system shown conceptually in Figure 2 is mathematically extensible to two-dimensions with an arbitrary number of crack and reinforcement directions. The equations of compatibility and equilibrium are satisfied by the overall framework of the GCCM; the constitutive laws for each of the distinct components (concrete, steel, and cracks) may be varied based on the best available models.

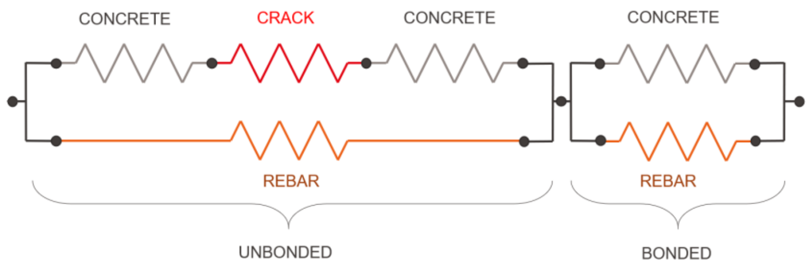

Figure 2. One-dimensional representation of cracked (unbonded) and uncracked (bonded) regions of reinforced concrete.

Although the GCCM is constructed as a general framework into which different constitutive laws can be inserted, in its original formulation, it also includes a simple behavioural model for cracks which has been shown to adequately capture the response exhibited in experiments. In this model, cracks are assumed to have tooth-like asperities that constrain opening and closing along a singular angle, denoted as the “tooth angle" α. This angle is defined by the crack width (w) and slip (δ), as shown in Figure 3. A quasi-rigid contact force may develop between the two lips of the crack if there is a shear on the crack. This contact force generally expressed as a normal component and a shear (friction) component; however, in comparison with observed experimental data it was found that the friction term is negligible and may be ignored. A similar assumption is made in the Contact Density Model for aggregate interlock of Le et al. (1989). Therefore, the contact force is assumed to act normal to the tooth angle.

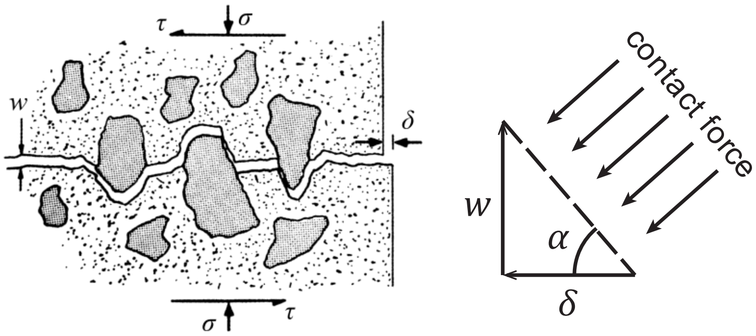

Figure 3. Kinematics of crack opening (after Vecchio & Collins (1986)).

The tooth angle at the moment of cracking is initially taken as 90°, but can degrade as the crack experiences interface shearing. In the GCCM this degradation is divided into two components:

1. Degradation under shear force as the crack widens. Termed the "dilatancy" or "monotonic" component, this degradation represents the effective change in contact angle as the width of the crack increases and crushing occurs at the tip of the tooth. This behaviour is taken to be similar in form to aggregate interlock relationships derived by others in the literature (Vecchio & Lai, 2004). The amount of angular degradation for a given shear force τ is given by:

$$\alpha_{mon} = \tan^{-1}(k_{mon} \cdot \tau) \quad (1)$$

   where k_{mon} is taken as 0.15 MPa^{-1}.

2. Degradation under cyclic loading. As the crack surface is cycled under constant load, it is hypothesized that there will be some erosion of the surfaces of the teeth, causing an effective decrease in the tooth angle. In the GCCM this degradation is modelled similar to Calvi et al. (2017) as proportional to the hysteretic energy dissipated through sliding on the tooth. In practice, since the frictional coefficient is taken as very small (approaching zero, as described above), the hysteretic energy becomes a measure of the total sliding path of the tooth. The decrease in angle is given by:

$$\alpha_{cyc} = \tan^{-1}(k_{cyc} \cdot U) \quad (2)$$

   where k_{cyc} is taken as 200 $(Nmm)^{-1}$ for members without confinement and U is the hysteretic energy dissipated on the crack tooth (calculated using a nominal friction coefficient of 0.001).

Taken together, the two degradation laws provide a reasonably accurate fit to experimentally derived observations.

2.2 Kinematic assessment method

The failure of cracked reinforced concrete under arbitrary loading may be generally classified as compressive failure or tensile/shear failure at the cracks. In the case of compression failure, observed laws describing compression softening provide an estimate of the reduction in compression capacity corresponding to transverse tensile strains (Vecchio & Collins, 1986). If the direction of principle compression is known, prediction of the residual compression capacity can be made on the basis of measured tensile strains due to coexisting cracking. Assessment of compression-governed structures is, however, outside the scope of this paper.

Failure at the crack interfaces may be formulated as the inability to find an equilibrium solution under at an applied load level. This will generally occur when the steel crossing the crack is yielding and the crack tooth cannot provide a sufficient reaction force to balance the other loads. The equilibrium at a crack will be studied for the case of general loading for panels reinforced in two orthogonal directions (notated x and z), subject to the tooth contact assumption of the GCCM. It is assumed that the crack is at a global angle of θ, which is not necessarily the angle corresponding to the current loading.

Under this idealized condition, for a given angle of the tooth, α, it is possible to illustrate the equilibrium of forces on the crack as shown in Figure 4 for a state of pure shear stress. While the reinforcing steel is in the elastic domain, the ratio between the force in the x-steel and z-steel will be related to the direction of the crack opening, defined by δ and w. The GCCM describes the compatibility conditions for these intermediate states. However, the present analysis will consider only the limit state in which both the x- and z-direction steel are reaching their yield limit (f_{yx} and f_{yz}, respectively). If both directions of steel are yielding, then for a known applied load state the force balance is completed by the contact force between the teeth.

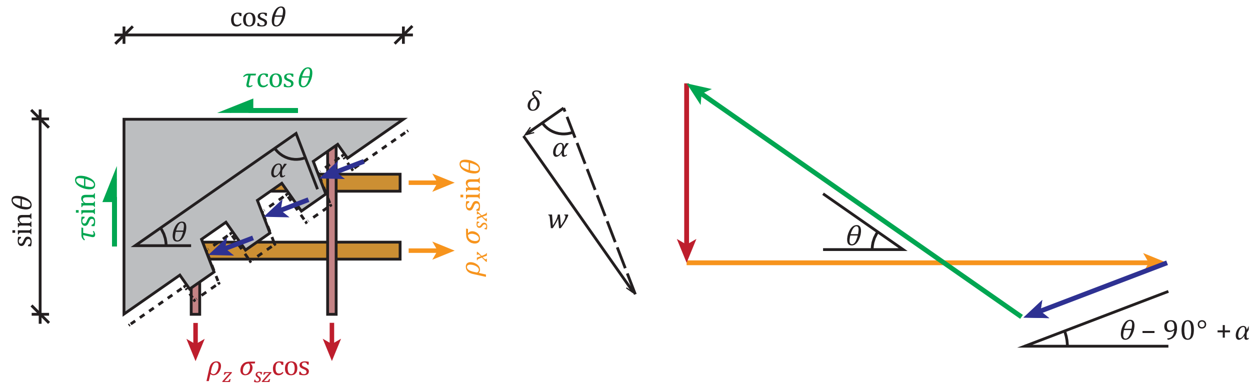

Figure 4. Free-body diagram at a crack (left); crack opening kinematics (middle); Cremona diagram for equilibrium of forces (right).

In the GCCM the contact force is not limited (there is no local crushing condition, for example; this is instead treated by crushing of the concrete in series with the crack); however, the angle of the contact force must be perpendicular to the crack tooth angle. If the tooth angle is too shallow, it is not possible to complete the force balance and find equilibrium. Therefore, for a given applied load state, one can determine the tooth angle at which the crack interface would fail. For angles steeper than this value, equilibrium is possible through a reduction in stress of the x-direction steel; the limit is reached when the tooth angle degrades and becomes too shallow.

For the case of pure shear as illustrated in Figure 4, one may write the following statement combining equilibrium in the x- and z- directions:

$$\tan(\theta - 90° + \alpha_{lim}) = \frac{\tau \sin\theta - \rho_y f_{yz} \cos\theta}{\rho_x f_{yx} \sin\theta - \tau \cos\theta} \quad (3)$$

Solving for α:

$$\alpha_{lim} = \tan^{-1}\left(\frac{\tau \sin\theta - \rho_y f_{yz} \cos\theta}{\rho_x f_{yx} \sin\theta - \tau \cos\theta}\right) + 90° - \theta \quad (4)$$

$$\alpha_{lim} = \tan^{-1}\left(\frac{\frac{\tau}{\rho_y f_{yz}} \sin\theta - \cos\theta}{\frac{\rho_x f_{yx}}{\rho_y f_{yz}} \sin\theta - \frac{\tau}{\rho_y f_{yz}} \cos\theta}\right) + 90° - \theta \quad (5)$$

A similar equilibrium statement can be made for the case where the applied normal stresses σ_x and σ_z are not equal to zero, though that case is not elaborated here.

This is a practical comparison to perform for assessment purposes, since the tooth angle is easily measured as the angle made by the crack slip and width components, as shown in Figure 3. Therefore, by comparing the observed crack opening angle to the theoretical limit angle computed for the applied loading, one obtains a measure of how imminent failure is. It should be noted that the rate of degradation of crack angle is not constant, so it is not possible to say, for example, that a tooth angle 5° away from failure always represents the same level of risk. However, for a number of cracks under similar loading and kinematic conditions, this gives a way of assessing the relative urgency with which they should be prioritized. The more general question of how close to failure a given crack is may be addressed using the full GCCM formulation and calculating the expected tooth angle degradation under monotonic or cyclic loading.

This limit state consideration provides a mechanical explanation and verification of the hypothesis first made by Stevens (1987) that reversed cyclic shear loading at the load level causing yield of the z-direction reinforcement will eventually cause failure. Using the tooth model, it becomes apparent that if the z-direction steel has yielded, then equilibrium is achieved through a balance between the x-direction steel force and the contact stress. As the tooth angle degrades (due to damage from cyclic loading) then the stress in the x-direction reinforcement must increase to compensate until the point when it cannot any longer (i.e., yield). At this moment the limit is reached and the crack interface is predicted to fail.

The degree of shear strength loss caused by reversed-cyclic loading is, therefore, not a fixed value, but depends on the number of cycles. With more cycles, a larger strength degradation is expected; that is, cycling at a lower stress amplitude will require more cycles to cause failure.

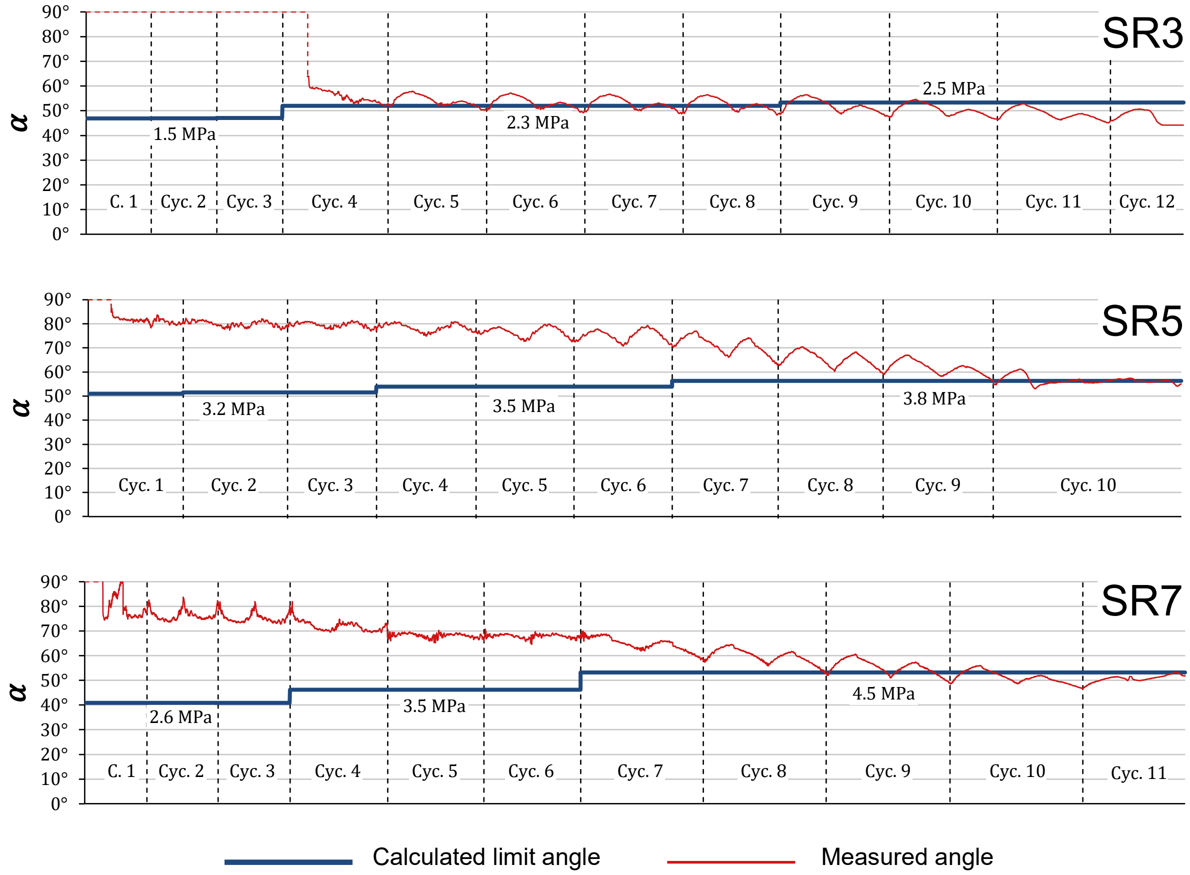

Figure 5. Degradation of crack tooth angle α and predicted limit angle.

2.3 Experimental validation

Validation of the procedure described above has been performed using three reversed cyclic shear experiments from the literature (Ruggiero, Bentz, Calvi, & Collins, 2016). In each of these experiments the load was cycled at increasing amplitudes until the point of failure. For each reversed cyclic shear amplitude τ, the corresponding theoretical limit angle α_{lim} has been calculated assuming a crack angle of $\theta = 45°$ corresponding to pure shear, and the known mechanical reinforcing ratios in the x- and z-directions. This limit angle has been plotted along with the measured average tooth angle, which itself was estimated through decomposition of the global strain state into crack slip and width components, as described in the referenced paper. The results are shown in Figure 5.

For all three experiments it can be seen that as the cycle amplitude increases the limit angle likewise increases. A larger limiting tooth angle indicates less reserve capacity, since it will take less degradation to reach that state. As the experiments progress the observed tooth angle decreases, and in each case, failure occurs approximately when the tooth angle reaches the calculated limit angle for that load level.

There are some uncertainties in the method that in some cases allow the observed angle to be lower than the theoretical limit. These include possible strain hardening of the steel reinforcement, friction on the cracks, and the possibility that the average crack angle was not precisely 45°. However, given the simplifications made, the calculated limit angle works as a sufficiently good indicator of proximity to failure.

3 Parametric study

3.1 Shear strength reduction under reversed cyclic loading

Based on the considerations above, it is evident that RC elements subjected to cyclic shear loading may not reach as high a strength as the same element subjected to monotonic shear. This is hypothesized to be due to the degradation of the crack tooth angle and the subsequent inability to keep equilibrium at a crack once the angle becomes too shallow. The strength reduction caused by cyclic loading is therefore not a fixed number but depends on the number of cycles; in theory one may cycle to failure at any load level, although subject to the assumptions of the GCCM, the amount of crack degradation is expected to be low before the z-direction reinforcement yields, in agreement with Stevens' hypothesis (1987).

One may quantify the possible amount of shear strength loss under cyclic loading by comparing the ultimate strength under monotonic loading to the stress level required to cause yield of the z-direction steel. Where this difference is large, members are at risk of experiencing a significant decrease in strength if subjected to cyclic loading. This can be a practical concern in cases where codes allow shear design based on monotonic formulations (Bentz, Vecchio, & Collins, 2006; Canadian Standards Association, 2019).

In order to identify regimes in which this shear strength degradation is most pronounced, a parametric analysis was conducted using the GCCM to compare predicted peak and yield strengths of panel elements. The main parameter of interest is the ratio between yield strength in the x- and z-directions (that is, $\rho_x f_{yx}/\rho_y f_{yz}$). Strain hardening was ignored; other parameters are reported together with the results on Figure 6.

Figure 6 illustrates how the addition of x-direction reinforcement increases the ultimate strength and yield strength at different rates. The ultimate strength reaches a plateau due to failure on the crack and crushing of concrete, while the yield strength increases with increasing $\rho_x f_{yx}$. As a result, the regime in which there is the most potential for cyclic degradation relative to the monotonic strength occurs around a ratio of 3.5 between the x- and z- direction steel strengths.

Figure 6 also plots Equation (5) as dashed lines. These lines indicate the strength as governed by equilibrium failure at a crack for fixed tooth angles; compression failure is not considered. In reality the tooth angle is expected to degrade significantly from 90° during loading, which is reflected in the GCCM ultimate strength prediction.

3.2 Prediction of cyclic failure using a fatigue framework

The strength degradation behaviour described above is similar to the fatigue observed in steel and other metallic materials under cyclic loading. As the stress level is decreased, the number of cycles to failure increases; however, below a certain limit unlimited or greatly increased cycling is possible without causing failure. A similar behaviour is predicted by the GCCM, and it is possible to run simulations at large numbers of cycles and many stress amplitudes to generate S-N curves to represent this as is typical for fatigue phenomena.

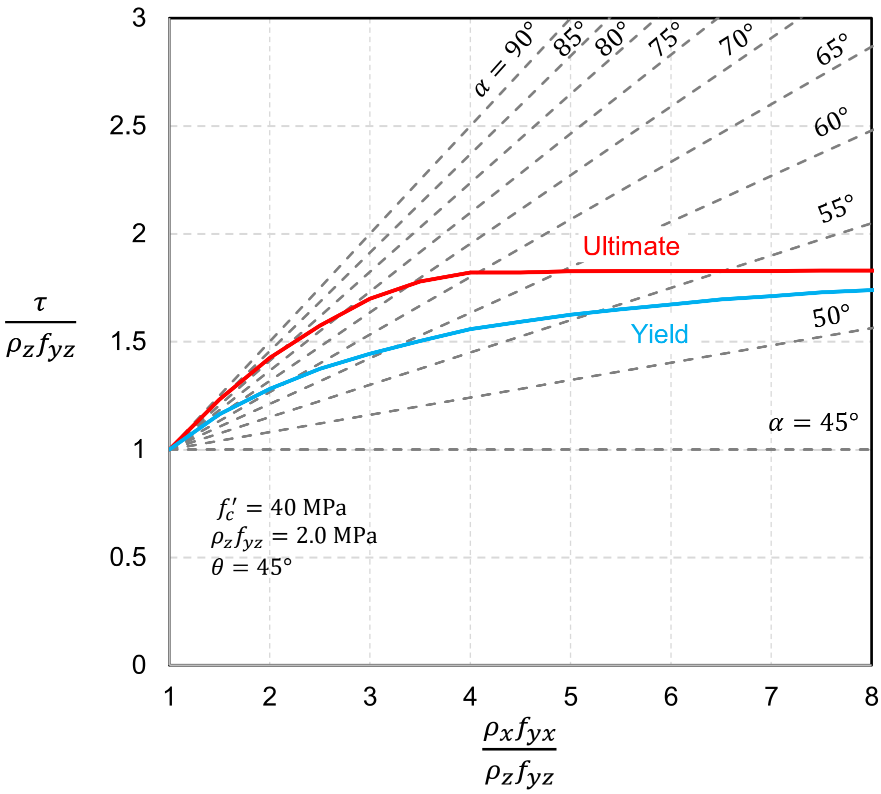

Figure 6. Difference between ultimate and yield strength of RC panel as function of reinforcing ratio, as predicted by the GCCM.

The hypothetical S-N curve for panel PV20 from the literature (Vecchio & Collins, 1986) has been generated and is shown in Figure 7. The curve, plotted on a log-log scale, has a decreasing regime and then a plateau, as predicted by the mechanical considerations. The decreasing part of the curve is not precisely linear, indicating that the behaviour in this regime does not follow a power function law. However, a lower bound linear limit can be easily fit to this data for easy adaption to design and assessment purposes.

The use of such S-N curves allows for a quantitative prediction of the number of cycles to failure at a given load level. It can also be used in an assessment context to determine the number of additional cycles to failure when the prior loading history is unknown but the tooth angle is measured; this requires additional information about the predicted crack tooth angle at each phase of cycling which could also be incorporated on such a plot.

As the crack tooth degradation mechanism in the GCCM is described by two empirical parameters (the dilatancy parameter k_{mon} and the cyclic degradation parameter k_{cyc}), a small sensitivity analysis has been conducted in which their values were varied from those initially proposed for the GCCM, as shown by the blue and red lines in Figure 7. The behaviour is relatively insensitive to the value of the cyclic parameter, but more sensitive in the low-cycle regime to the dilatancy parameter. Further research is required to better determine these constants.

It should be emphasized that no experimental data exists for RC panels subjected to high-cycle fatigue, so it is difficult to verify these predictions. Only relatively low-cycle experiments are available in the literature, and it is from these tests that the degradation parameters of the GCCM have been fit, therefore there is considerable uncertainty in extrapolation. Nonetheless, this example demonstrates how the framework of the GCCM predicts a behaviour with these characteristics. Improved modelling of the interface degradation law and verification with experiments with large numbers of cycles in the future will allow for validation of this hypothesis and the generation of practical S-N curves for assessment of cyclic loading on RC structures.

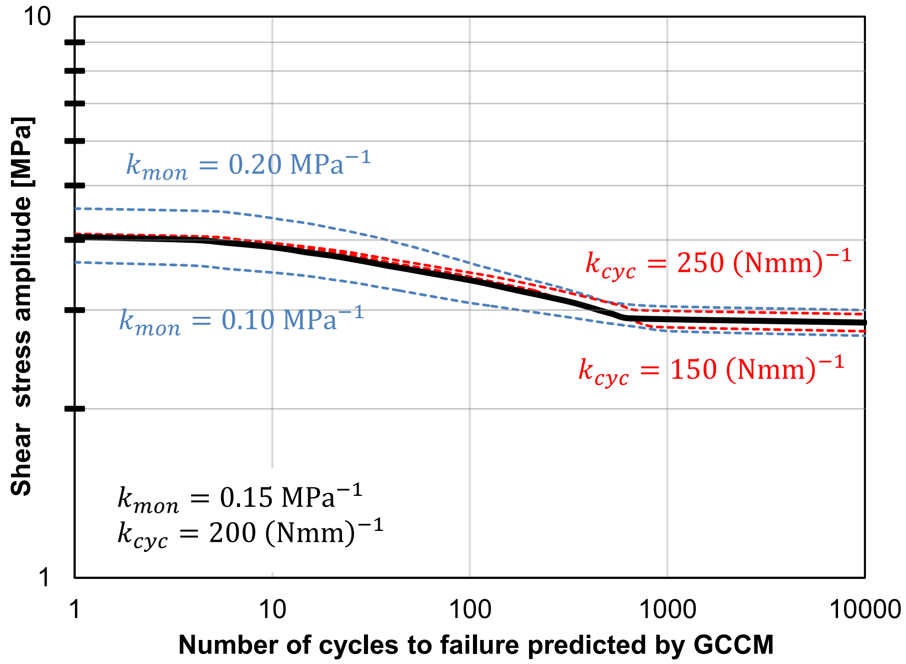

Figure 7. Sample S-N curve as predicted by GCCM, showing sensitivity to parameters k_{mon} and k_{cyc}.

4 Conclusion

This study has investigated the behavior of RC elements subjected reversed cyclic shear loading, with a particular focus on shear strength reduction due to failure at the cracks. The GCCM has provided a simple, mechanics-based framework for this analysis, allowing exploration of the impact of crack kinematics (width and slip) on shear failure under different reinforcement ratios.

As has been previously demonstrated experimentally, cyclic loading of RC elements can result in significant reductions in shear strength. This work has shown how the strength reduction can be related to the degradation of the crack teeth. A kinematic assessment method was proposed, by which the proximity to failure is estimated by comparing the measured crack opening angle with a theoretical limit. This approach provides a valuable tool for assessing the condition and potential risk of existing reinforced concrete structures exposed to cyclic loading.

Regimes where shear strength degradation under cyclic loading is most pronounced were identified through parametric analysis. A critical factor was found to be the ratio between the yield strength of the x-direction and z-direction steel, with a ratio of approximately 3.5 representing a region of heightened vulnerability to cyclic degradation. To represent the fatigue-like behavior predicted by the GCCM degradation model, ax example S-N curve was generated as a way of predicting the number of cycles to failure at different load levels.

While the predictions put forward in this paper are based on theoretical assumptions and require further validation through experimental data, they provide insights into the cyclic behavior of reinforced concrete elements. Future research, including experimental studies with high-cycle fatigue data, is needed to refine and validate the proposed models and parameters.

In summary, this study contributes to our understanding of shear strength reduction in reinforced concrete under cyclic loading and provides a framework for the assessment of damaged structures using simple, mechanical models. It is our hope that this research will inform and enhance the safety and reliability of reinforced concrete structures in the face of loading from severe events such as earthquakes.

5 References

Bentz, E. C., Vecchio, F. J., & Collins, M. P. (2006). Simplified Modified Compression Field Theory for Calculating Shear Strength of Reinforced Concrete Elements. *ACI Structural Journal, 103*(4), 614-624.

Birrcher, D., Tuchscherer, R., Huzinga, M., Bayrak, O., Wood, S., & Jirsa, J. (2009). *Strength and Serviceability Design of Reinforced Concrete Deep Beams, Rep. No. 0-5253-1.* Austin: Center for Transportation Research, The University of Texas at Austin.

Calvi, P. M., Bentz, E. C., & Collins, M. P. (2017). Pure Mechanics Crack Model for Shear Stress Transfer in Cracked Reinforced Concrete. *ACI Structural Journal, 114*(2), 545-554.

Calvi, P. M., Proestos, G. T., & Ruggiero, D. M. (2018). Towards the development of direct crack-based assessment of structures. *ACI SP-328: Shear in structural concrete*, 9.1-9.9.

Campana, S., Fernandez Ruiz, M., Anastasi, A., & Muttoni, A. (2013). Analysis of shear-transfer actions on one-way RC members based on measured cracking pattern and failure kinematics. *Magazine of Concrete Research, 65*(6), 386-404.

Canadian Standards Association. (2019). *Design of Concrete Structures (CSA A23.3:19).* Mississauga: Canadian Standards Association.

Cavagnis, F., Fernández Ruiz, M., & Muttoni, A. (2017). An analysis of the shear-transfer actions in reinforced concrete members without transverse reinforcement based on refined experimental measurements. *Structural Concrete, 19*(1), 49-64.

Červenka, J., Červenka, V., & Laserna, S. (2018). On crack band model in finite element analysis of concrete fracture in engineering practice. *Engineering Fracture Mechanics, 197*, 27-47.

Collins, M. P., Bentz, E. C., Quach, P. T., & Proestos, G. T. (2015). The Challenge of Predicting the Shear Strength of Very Thick Slabs. *Concrete International, 37*(11), 29-37.

Hillerborg, A., Modéer, M., & Petersson, P.-E. (1976). Analysis of crack formation and crack growth in concrete by means of fracture mechanics and finite elements. *Cement and Concrete Research, 6*(6), 773-781.

Lantsoght, E. O., van der Veen, C., Walraven, J. C., & de Boer, A. (2016). Case Study on Aggregate Interlock Capacity for the Shear Assessment of Cracked Reinforced-Concrete Bridge Cross Sections. *Journal of Bridge Engineering, 21*(5).

Larson, N., Gomez, E. F., Garber, D., Bayrak, O., & Ghannoum, W. (2013). *Strength and serviceability design of reinforced concrete inverted-T beams. Rep. No. FHWA/TX-13/0-6416-1.* Austin: Center for Transportation Research - The University of Texas at Austin.

Li, B., Maekawa, K., & Okamura, H. (1989). Contact density model for stress transfer across cracks in concrete. *Journal of the Faculty of Engineering, 40*(1), 9-52.

Mihaylov, B. I., Bentz, E. C., & Collins, M. P. (2013). Two-Parameter Kinematic Theory for Shear Behavior of Deep Beams. *ACI Structural Journal, 110*(3), 447-456.

Palermo, D., & Vecchio, F. J. (2007). Simulation of Cyclically Loaded Concrete Structures Based on the Finite-Element Method. *ASCE Journal of Structural Engineering, 133*(5), 728-738.

Ruggiero, D. M. (2015). *The Behaviour of Reinforced Concrete Subjected to Reversed Cyclic Shear.* Toronto: Ph.D. Thesis, University of Toronto.

Ruggiero, D. M., Bentz, E. C., Calvi, G., & Collins, M. P. (2016). Shear Response under Reversed Cyclic Loading. *ACI Structural Journal, 113*(6), 1313-1324.

Ryan, T. W., Mann, J. E., Chill, Z. M., & Ott, B. T. (2012). *Bridge Inspector's Reference Manual (BIRM).* Arlington: U.S. Department of Transportation, Federal Highway Administration.

Sain, T., & Chandra Kishen, J. M. (2007). Residual fatigue strength assessment of concrete considering tension softening beahviour. *International Journal of Fatigue, 29*(12), 2138-2148.

Stevens, N. J. (1987). *Analytical modelling of reinforced concrete subjected to monotonic and reversed loadings.* Toronto: Ph.D. dissertation, University of Toronto, Department of Civil Engineering.

Trandafir, A. N., Proestos, G. T., & Mihaylov, B. I. (2022). Detailed crack-based assessment of a 4-m deep beam test specimen. *Structural Concrete, 24*(1), 756-770.

Vecchio, F. J., & Collins, M. P. (1986). The modified compression-field theory for reinforced-concrete elements subjected to shear. *Journal of the American Concrete Institute, 83*(2), 219-231.

Vecchio, F. J., & Lai, D. (2004). Crack Shear-Slip in Reinforced Concrete Elements. *Journal of Advanced Concrete Technology, 2*(3), 289-300.

Wang, J., Shi, Z., & Nakano, M. (2013). Strength degradation analysis of an aging RC girder bridge using FE crack analysis and simple capacity-evaluation equations. *Engineering Fracture Mecahnics, 108*, 209-221.

Zaborac, J., Athanasiou, A., Salamone, S., Bayrak, O., & Hrynyk, T. D. (2020). Crack-based shear strength assessment of reinforced concrete members using a fixed-crack continuum modeling approach. *Journal of Structural Engineering, 146*(4), 04020024.

Zaborac, J., Perez, B., Hrynyk, T., & Bayrak, O. (2020). Structural performance assessment of a 60-year-old reinforced concrete bent cap. *Structural Concrete, 21*(6), 2549-2564.

Zhai, J., Chen, C. I., Worsfold, B. L., & Moehle, J. P. (2022). Blind Prediction Competition of a Full-Scale Shear-Critical Reinforced Concrete Mat Foundation Slice. *Proceedings of the 12th National Conference on Earthquake Engineering.* Salt Lake City: Earthquake Engineering Research Institute.

Zhu, R., Wanichakorn, W., Hsu, T., & Vogel, J. (2003). Crack width prediction using compatibility-aided strut-and-tie model. *ACI Structural Journal, 100*(4), 413-421.